Polarization charge distribution in gapped graphene: Perturbation theory and exact diagonalization analysis

Valeri N. Kotov, Vitor M. Pereira, and Bruno Uchoa
Department of Physics, Boston University, 590 Commonwealth Avenue, Boston, Massachusetts 02215, USA
(Received 6 June 2008; revised manuscript received 4 August 2008; published 22 August 2008)

We study the distribution of vacuum polarization charge induced by a Coulomb impurity in massive graphene. By analytically computing the polarization function, we show that the charge density is distributed in space in a nontrivial fashion and on a characteristic length-scale set by the effective Compton wavelength. The density crosses over from a logarithmic behavior below this scale to a power-law variation above it. Our results in the continuum limit are confirmed by explicit diagonalization of the corresponding tight-binding model on a finite-size lattice. Electron-electron interaction effects are also discussed.

DOI: 10.1103/PhysRevB.78.075433 PACS number(s): 81.05.Uw, 73.43.Cd

I. INTRODUCTION AND FORMULATION OF THE PROBLEM

Over the course of the past year the behavior of graphene in the presence of a strong external Coulomb field was analyzed in considerable detail.[1–6] This problem is important, notably, for our understanding of electronic transport in the presence of charged impurities.[7] In addition, since the effective coupling constant in graphene $\alpha=e^2/(\hbar v)$ can be rather large (in vacuum $\alpha=2.2$), the exploration of features uniquely associated with the strong-field regime $Z\alpha\sim 1$ [where Z stands for the strength of the external Coulomb field $V(r)=Ze/r$] becomes a realistic prospect. In this context, it was found that above a critical value $(Z\alpha)_c=1/2$ characteristic resonances appear in the energy spectrum[1,2] and the vacuum polarization density varies as $\rho(\mathbf{r})\sim 1/r^2$. In the subcritical regime $(Z\alpha<1/2)$, on the other hand, the polarization charge is concentrated around the Coulomb center in such a way that one obtains $\rho(\mathbf{r})\propto\delta(\mathbf{r})$ within the continuum approximation for the electron dynamics. The physics around the critical point $(Z\alpha)_c$ is a peculiar massless realization of the more "conventional" vacuum charging behavior in massive quantum electrodynamics (QED)[8] which also seems possible in graphene under certain conditions.[6]

The drive to explore unconventional behavior at strong coupling $(Z\alpha\sim 1)$ has been fueled, so far, by theoretical progress only. Experiments in which K^+ ions are deposited in a controlled way onto graphene show the behavior one expects from the theory of scattering of Dirac fermions by a Coulomb field,[9,10] but only in the undercritical regime, perhaps as expected for such low value of Z. It is also clear that under current experimental conditions $\alpha<1$ due to dielectric screening by the substrate, and additional screening is provided by the presence of water layers around the samples.[11] This conspires to significantly increase the effective dielectric constant with a concomitant decrease of α, thus making the subcritical regime $Z\alpha<(Z\alpha)_c$ the relevant one for present-day experiments, and also accounting for the feeble signatures of interaction effects. It is therefore natural to ask how the characteristic features of the undercritical regime manifest themselves in the vacuum polarization and screening properties. In the strict massless limit the polarization charge density is concentrated at the potential source $\rho(\mathbf{r})\propto Z\alpha\delta(\mathbf{r})$ and nontrivial spatial variation can only occur due to additional interaction effects.[3] These are expected to be small and we will see that, perturbatively, they read $\rho(\mathbf{r})\sim Z\alpha^2/r^2$.

In the present work we explore another source of density variation caused by the presence of a finite "mass" m or, equivalently, an energy gap $\Delta=2mv^2$ in the electronic spectrum. There are at least three sources of a gap in graphene. First, it has been realized recently[12] that epitaxially grown graphene exhibits a substantial gap ($\Delta=0.26$ eV) due to the breaking of the sublattice symmetry by the substrate. Graphene suspended above a graphite substrate also has a small gap $\Delta\approx 10$ meV.[13] Second, spin-orbit coupling leads to a gap, albeit of much smaller magnitude $\Delta_{so}\simeq 10^{-3}$ meV.[14] Finally, real mesoscopic samples can have an effective gap generated by their finite size, which scales as $\Delta\sim 1/L$. We find that the polarization density of massive Dirac fermions displays characteristic behavior, controlled by the effective "Compton" wavelength $\lambda_C=\hbar/(mv)$. Our main results are summarized in Figs. 3 and 4; for distances $r\lesssim\lambda_C$, the density variation is logarithmic, crossing over to a power-law tail at $r\gtrsim\lambda_C$. It should be possible to explore this behavior with modern experimental techniques for detection of local-density variation.[13,15,16]

Our starting point is a two-dimensional (2D) system of massive Dirac electrons in the presence of a Coulomb impurity with effective charge Ze. The Hamiltonian is

$$\hat{H}=-i\hbar v\boldsymbol{\sigma}\cdot\nabla+mv^2\sigma_3-\frac{Ze^2}{r},\tag{1}$$

where v is the Fermi velocity and σ_i are the Pauli matrices. The induced vacuum polarization charge is calculated in linear response according to

$$\rho(\mathbf{q})=ZeV(\mathbf{q})\Pi(\mathbf{q},0),\quad V(\mathbf{q})=\frac{2\pi\alpha}{|\mathbf{q}|},\tag{2}$$

where $\alpha=e^2/(\hbar v)$ and $\Pi(\mathbf{q},0)$ is the static polarization function. This equation is schematically represented by the diagram in Fig. 1.

Unless specified otherwise, we use units in which $v=\hbar=1$, the electron charge is $-e$ $(e>0)$, and, for convenience, we measure all charges (ρ,Q) in units of e (the sign is mean-

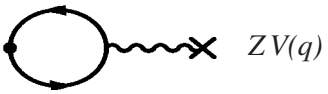

FIG. 1. Graphical representation of Eq. (2).

ingful though). The chemical potential μ is assumed to be in the gap $|\mu|<m$ (further discussion appears later).

In the rest of the paper, we first compute the polarization operator for massive graphene (Sec. II), which we use in Sec. III for the calculation of the induced vacuum polarization charge in a weak Coulomb field. In Sec. IV we compare the obtained behavior with results based on exact diagonalization studies on a finite-size lattice. Section V discusses the influence of weak electron-election interactions on the polarization charge, and Sec. VI contains our conclusions.

II. POLARIZATION FUNCTION FOR MASSIVE DIRAC PARTICLES

The polarization function is computed in the standard way as

$$\Pi(\mathbf{q},\omega) = -iN\sum_{\mathbf{k}} \int \frac{d\nu}{2\pi} \mathrm{Tr}\{\hat{G}(\mathbf{k},\nu)\hat{G}(\mathbf{k}+\mathbf{q},\nu+\omega)\}, \quad (3)$$

where the trace is over the Pauli matrices and $N=4$ accounts for the valley and spin degeneracies. The Green's function at finite mass is given by

$$\hat{G}(\mathbf{k},\nu) = \frac{\nu + \boldsymbol{\sigma}\cdot\mathbf{k} + m\sigma_3}{\nu^2 - \mathbf{k}^2 - m^2 + i\eta}. \quad (4)$$

Using a more symmetric three-vector notation, $(\mathbf{q},q_0)=(\mathbf{q},\omega)$, $(\mathbf{k},k_0)=(\mathbf{k},\nu)$, $k^2=\mathbf{k}^2-k_0^2$, etc., we obtain

$$\Pi(\mathbf{q},q_0) = -8i\int \frac{d^3k}{(2\pi)^3} \frac{k_0(k_0+q_0)+\mathbf{k}\cdot(\mathbf{k}+\mathbf{q})+m^2}{(k^2+m^2)[(k+q)^2+m^2]}. \quad (5)$$

Technically, an exact analytical evaluation of Eq. (5) becomes possible if one treats the frequency and momentum integrations on equal footing, as would happen in a Lorentz invariant situation and was done for the massless case.[17] However in this way one encounters a linearly divergent piece, since it is clear that at large momenta Eq. (5) leads to $\int^{\Lambda} d^3k/k^2 \sim \Lambda$, where Λ is the covariant ultraviolet cutoff. This procedure therefore requires "regularization," i.e., subtraction of the infinite contribution. The regularization procedure, however, yields the correct result because in a nonrelativistic situation, when the energy (k_0) integration is performed first in the interval $(-\infty,\infty)$, the resulting momentum integration is ultraviolet convergent (and cutoff independent).

Restoring the original notation, we obtain the final exact expression for the polarization

$$\Pi(\mathbf{q},\omega) = -\frac{|\mathbf{q}|^2}{\pi}\left\{\frac{m}{q^2} + \frac{1}{2q}\left(1-\frac{4m^2}{q^2}\right)\arctan\left(\frac{q}{2m}\right)\right\}, \quad (6)$$

where

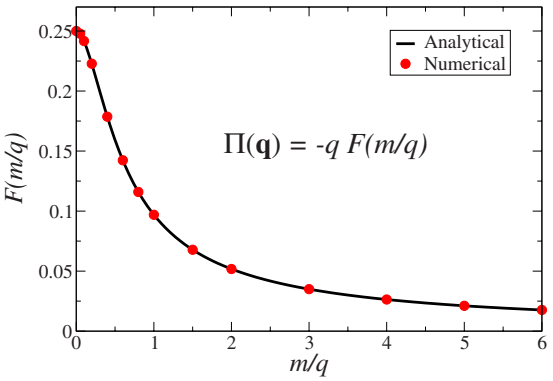

FIG. 2. (Color online) Plot of the function $F(m/q)$, defined as $\Pi(\mathbf{q},\omega=0)=-qF(m/q)$, where $q=|\mathbf{q}|$.

$$q = \sqrt{|\mathbf{q}|^2 - \omega^2}. \quad (7)$$

Unlike QED, the polarization function of graphene is not covariant. We have confirmed this result by direct numerical integration of Eq. (3). A comparison of the two in the static case ($\omega=0$) is shown in Fig. 2, where the correspondence between the numerical calculation and Eq. (6) is exact.

At finite frequency, dynamical properties such as the longitudinal conductivity of gapped graphene can be derived directly from Eq. (6). For the real part of the conductivity $\sigma_m(\omega)$ one can use the standard formula $\sigma_m(\omega)=-e^2(\omega/\mathbf{q}^2)\mathrm{Im}\,\Pi(\mathbf{q},\omega)$ (Ref. 18) for $|\mathbf{q}|\to 0$. We readily extract the imaginary part of the dynamical polarization

$$\mathrm{Im}\,\Pi(\mathbf{q},\omega) = \frac{-|\mathbf{q}|^2}{4\tilde{q}}\left\{1+\frac{4m^2}{\tilde{q}^2}\right\}\theta(\omega-\sqrt{|\mathbf{q}|^2+4m^2}), \quad (8)$$

where we define

$$\tilde{q} \equiv \sqrt{\omega^2 - |\mathbf{q}|^2}. \quad (9)$$

This leads to

$$\frac{\sigma_m(\omega)}{\sigma_0} = \left(1+\frac{4m^2}{\omega^2}\right)\theta(\omega-2m), \quad (10)$$

where σ_0 is the conductivity of massless graphene, predicted to be $\sigma_0=e^2/(4\hbar)$.[7] Equation (10) implies that, at the edge $\omega=2m$, the conductivity increases by a factor of two $\sigma_m=2\sigma_0$ and decreases for higher frequencies, approaching $\sigma_m=\sigma_0$ ($\omega\gg m$). For a gap of $\Delta=2m\approx 260$ meV,[12] we estimate that the characteristic frequencies where the enhancement should be observable are $\omega\sim\Delta\sim 2\times 10^3$ cm^{-1}, which are typical frequencies in infrared spectroscopy.[19] Similar effects were previously discussed in magnetotransport (in particular when a gap is opened in strong magnetic field).[20]

III. INDUCED VACUUM POLARIZATION CHARGE

In the following discussion, we assume $\omega=0$ ($q=|\mathbf{q}|$) and denote $\Pi(\mathbf{q})=\Pi(\mathbf{q},0)$. First we extract the behavior in some limiting cases. In the limit of large momenta we have

$$\Pi(\mathbf{q}) = -q\left(\frac{1}{4}-\frac{m^2}{q^2}\right), \quad \frac{q}{m}\gg 1, \quad (11)$$

whereas in the opposite limit

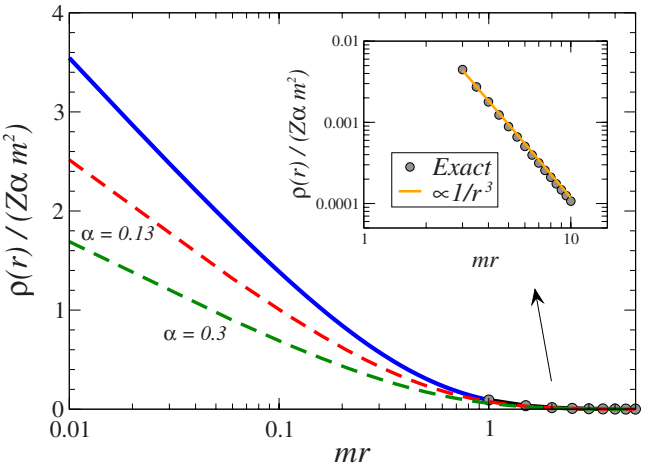

FIG. 3. (Color online) Polarization charge from Eq. (13) (solid line). The effect of additional electron-electron interactions (within RPA as discussed in the text) is also shown (dashed lines). Inset: magnification of the $1/r^3$ behavior at large distances.

$$\Pi(\mathbf{q}) = -\frac{q^2}{3\pi m}, \quad \frac{q}{m} \ll 1. \tag{12}$$

These limits determine the behavior of the polarization charge at small and large distances, respectively, which we proceed to investigate in more detail.

The distribution of the polarization charge density in real space is given by

$$\rho(\mathbf{r}) = Z\int \frac{d^2\mathbf{q}}{(2\pi)^2} V(\mathbf{q})\Pi(\mathbf{q})e^{i\mathbf{q}.\mathbf{r}}. \tag{13}$$

On the scale of the lattice spacing a away from the impurity there is a contribution to the screening charge that reads

$$\rho(\mathbf{r}) = -Z\alpha\frac{\pi}{2}\delta(\mathbf{r}), \quad r \simeq a \to 0, \tag{14}$$

which is valid in the continuum limit ($a \to 0$) and comes from the linear contribution in Eq. (11). In the massless situation ($m=0$) this localized polarization charge is the final result. The finite mass introduces new behavior, namely, additional polarization charge appears distributed in space. The full behavior of $\rho(\mathbf{r})$ is shown in Fig. 3 (solid blue line). One clearly identifies two distinct regimes whose asymptotic regions are determined by the Compton wavelength, the characteristic length scale of the problem

$$\lambda_C = \frac{\hbar}{mv} \to \frac{1}{m}(\hbar = v = 1). \tag{15}$$

Using Eqs. (11) and (12), for distances much smaller than λ_C (yet away from the Dirac delta at $r=0$) we find logarithmic decay

$$\rho(\mathbf{r}) \sim Z\alpha m^2 \ln\left(\frac{1}{mr}\right), \quad ma \ll mr \ll 1, \tag{16}$$

while at large distances a *fast* power law emerges[21]

$$\rho(\mathbf{r}) \sim Z\alpha m^2 \frac{1}{(mr)^3}, \quad mr \gg 1. \tag{17}$$

These two regimes are evidenced in Fig. 3 by means of the log scale in the main panel [cf. Eq. (16)] and by the fit shown in the inset [cf. Eq. (17)]. The numerical evaluation of Eq. (13) shown in the figure provides the crossover between the two asymptotic regimes.

It is also significant to notice that the two contributions—the localized term (14) and the spread tail—have different signs: the lattice-scale contribution has a screening sign, while the long-range tail has a compensating, *antiscreening* sign. This follows from the fact that, per Eq. (12), $\rho(q=0)=0$, meaning that the total polarization charge $Q(\infty)=0$, where $Q(R)$ is the vacuum charge accumulated within radius R:

$$Q(R) = \int_{|\mathbf{r}|<R} \rho(\mathbf{r})d\mathbf{r}. \tag{18}$$

In fact, the rapid decay of $\rho(\mathbf{r})$ beyond λ_C means that most of the additional (positive) charges compensating Eq. (14) are accumulated between the lattice scale ($r \simeq a$) and λ_C, in such a way that $Q(R \gtrsim 1/m) \approx 0$. This has peculiar consequences for screening: the impurity potential is best screened at the shortest distances ($r \simeq a$), screening weakens between $a \lesssim r \lesssim \lambda_C$, and is essentially absent beyond λ_C. Thus the impurity charge remains unscreened at large distances, as expected for an insulator.

IV. INDUCED CHARGE ON A FINITE LATTICE

To confirm the applicability of the above results to the real problem on a lattice and to dismiss possible regularization issues, we have investigated via exact diagonalization the corresponding tight-binding model for graphene, where the lattice appears naturally. The induced charge density can be straightforwardly obtained with the aid of the exact wave functions

$$\rho(\mathbf{r}) = -\sum_{E\le -m} \Psi_E^\dagger(\mathbf{r})\Psi_E(\mathbf{r}) + \sum_{E\le -m} \Psi_E^{0\dagger}(\mathbf{r})\Psi_E^0(\mathbf{r}). \tag{19}$$

Summation over the two spin components is also assumed (leading to an additional factor of 2). Here Ψ_E^0 are the wave functions without external field ($Z=0$). Rather than address the induced charge itself, it is more convenient to consider $Q(R)$ as defined in Eq. (18). This quantity is already averaged over all directions and is thus smoother and more appropriate for a direct numerical comparison.

We have studied two cases: (a) tight-binding model on a finite lattice with 124×124 sites, without explicit mass term, and (b) the same system with an explicit mass of $mv^2 = 0.1t$, where t is the hopping parameter. These two cases allow us to address the two asymptotic regimes in Eqs. (16) and (17). In case (a), although m is explicitly zero, there is an effective gap due to the finite size of the system $2mv^2 = \Delta \simeq 0.06t$ and an effective $\lambda_C \simeq 50a$.[6] Therefore, there is an appreciable region satisfying $a \lesssim r \lesssim \lambda_C$. The calculated $Q(R)$ for this case is shown in Fig. 4(a). Its behavior consists of a sharp in-

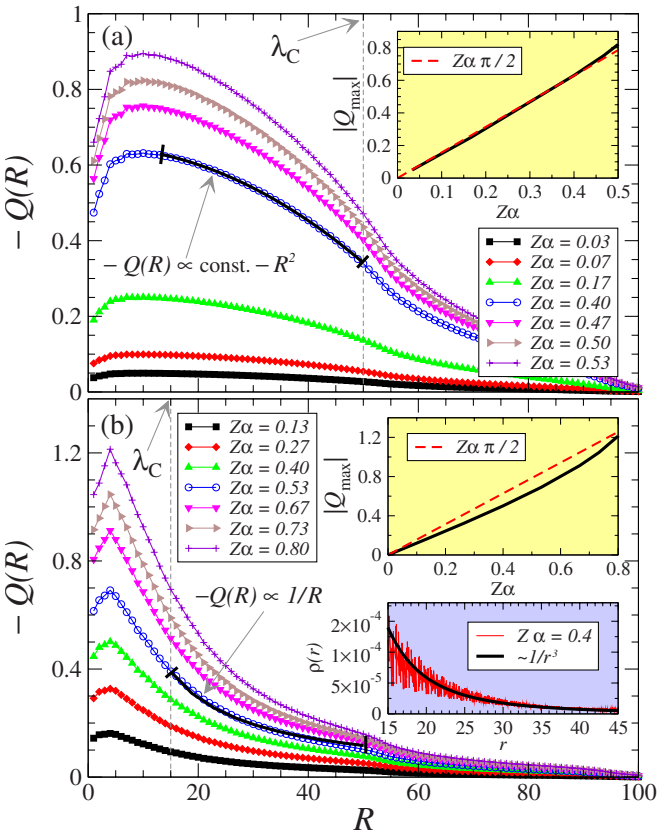

FIG. 4. (Color online) Exact diagonalization plots of $Q(R)$, Eq. (18), in the subcritical regime (we set $a=1$ in the plot). (a) Finite-size gap only, with $\lambda_C \simeq 50$. (b) Explicit mass $mv^2=0.1t$, leading to $\lambda_C \simeq 15$. In both cases, the apparent inflections at $R \simeq 55$ are due to boundary effects of the finite system. The top insets compare the maximum of $Q(R)$ ($Q_{\max}$) obtained in the lattice with the value expected from Eq. (14).

crease for $R \sim a$ and a subsequent slow decay up to λ_C. This decay follows the law $-Q(R) \propto (\text{const.} - R^2)$, as one expects from Eq. (16). Unfortunately, for our system $R=55a \approx \lambda_C$ is the largest distance from the impurity that is free from boundary effects, and one cannot comment on the crossover at larger distances. In order to address that limit we look at case (b), for which λ_C is much smaller ($\lambda_C \approx 15a$); our results are shown in Fig. 4(b). In effect, we obtain $Q(R) \propto R^{-1}$ in the region $r \gtrsim \lambda_C$, in accordance with the result in Eq. (17). In the lower inset of the figure we show the r^{-3} decay of the actual induced charge on the lattice, for a particular value of the coupling. The smallness of λ_C in this case means that the intermediate, logarithmic, regime is inaccessible. The analytical behavior thus stands in the lattice problem, with qualitative and quantitative agreements, even for the case when the gap is due to the finite lattice size.

V. ROLE OF ELECTRON-ELECTRON INTERACTIONS

Electron-election interactions can influence the behavior described above. Although questionable on account of the strict zero carrier density, one can perform resummation of polarization loops within the random-phase approximation (RPA). For weak interactions RPA is expected to work quantitatively well, with deviations increasing as the interaction α increases.[22] RPA amounts to the substitution $\Pi(\mathbf{q}) \rightarrow \Pi(\mathbf{q})/[1-V(\mathbf{q})\Pi(\mathbf{q})]$ in Eq. (13). The outcome of this procedure is given in Fig. 3 for different values of the interaction, being clear that the result is a small decrease in the coefficient of the log in Eq. (16).

In addition, a qualitatively important effect arises from self-energy corrections to the polarization. We evaluate the self-energy at Hartree-Fock level, which was first done for the massless case in Ref. 23. In the massive case we obtain a velocity renormalization of

$$v \rightarrow v(q) = v\left\{1 + \frac{\alpha}{4}\ln\left(\frac{\Lambda + \sqrt{\Lambda^2 + m^2}}{q + \sqrt{q^2 + m^2}}\right)\right\}, \qquad (20)$$

where $\Lambda \sim 1/a$ is the ultraviolet cutoff and the above expression is valid for $q, m \ll \Lambda$. The mass is also renormalized to a larger value $\tilde{m}$:

$$m \rightarrow \tilde{m} = m\left\{1 + \frac{\alpha}{2}\ln\left(\frac{\Lambda}{m}\right)\right\}, \quad m \ll \Lambda. \qquad (21)$$

It is interesting to note that the logarithmic mass-renormalization formula in graphene (21) is similar to the well-known expression for the electromagnetic mass (accounting for radiative corrections) in three-dimensional relativistic QED.[24,25]

From Eq. (20), for $\Lambda \gg q \gg m$, one has $v \rightarrow v(q) = v[1 + \frac{\alpha}{4}\ln(\Lambda/q)]$, which leads to the "running" of the coupling constant $\alpha(q) = e^2/v(q)$. Consequently, expanding $v(q)$ in powers of α leads, perturbatively, to an additional piece in the polarization charge

$$\delta\rho(r) \sim \frac{Z\alpha^2}{16}\frac{1}{r^2}, \quad a < r < 1/m. \qquad (22)$$

This is the perturbative limit of the effect, as discussed in Ref. 3.

We conclude that electron-electron interactions affect somewhat the above discussed behavior at the scale λ_C, but do not change the picture qualitatively. This can be credited to the mentioned absence of screening and the fact that interactions do not generate an additional length scale. Furthermore, it seems that in current experiments $\alpha \ll 1$ making the interaction corrections parametrically small.

VI. CONCLUSIONS

We have found that in the presence of a finite mass gap the polarization charge, induced by a Coulomb impurity in graphene, has a nontrivial behavior as a function of distance. While at zero mass it is concentrated at the impurity site; at finite mass it is distributed mostly up to $\lambda_C = 1/m$, with an additional power-law tail beyond that. Unlike the massless case, the total vacuum charge is zero since the finite mass "pulls" a compensating charge from infinity to a distance $\sim \lambda_C$, and the impurity charge remains unscreened beyond this scale.

In relativistic QED (Ref. 25) the polarization charge at short distances has antiscreening sign (enhances the poten-

tial), while the compensating charge is distributed up to the Compton wavelength of the electron. This behavior arises from the running of the charge $e^2(r)$ in QED. In nonrelativistic graphene (where the charge is not renormalized), the situation is reversed as shown by the sign of Eqs. (14), (16), and (17).

In the experiment of Ref. 12, where the spectral gap is $\Delta \approx 0.26$ eV, we have $\lambda_C \approx 30a \approx 4$ nm and the behavior we predict in this work should be observable if an external ion is present and generates the discussed charge redistribution. In practical terms, in order to detect the density variation the chemical potential might have to be at or above the value of the gap $|\mu| \geq m$. Our results will then be strictly valid only for $|\mu| \gtrsim m$, where the screening length (determined by the occupation of the conduction band) remains large and well separated from the scale λ_C. Although we strictly have a hyperbolic band, when $|\mu| \gtrsim m$ we can resort to the behavior of a parabolic band in 2D. Screening in this case is somewhat peculiar[26] due to the finite density of states at the band edge $N(\mu=m) \propto m$. We expect that this could in fact facilitate detection of density variations via scanning tunnel microscope (Refs. 13 and 16) compared to the massless case in graphene.

ACKNOWLEDGMENTS

We are grateful to A. H. Castro Neto and O. P. Sushkov for many stimulating discussions. V.M.P. was supported by FCT via Contract No. SFRH/BPD/27182/2006.

[1] V. M. Pereira, J. Nilsson, and A. H. Castro Neto, Phys. Rev. Lett. **99**, 166802 (2007).
[2] A. V. Shytov, M. I. Katsnelson, and L. S. Levitov, Phys. Rev. Lett. **99**, 236801 (2007); **99**, 246802 (2007).
[3] R. R. Biswas, S. Sachdev, and D. T. Son, Phys. Rev. B **76**, 205122 (2007).
[4] I. S. Terekhov, A. I. Milstein, V. N. Kotov, and O. P. Sushkov, Phys. Rev. Lett. **100**, 076803 (2008).
[5] M. M. Fogler, D. S. Novikov, and B. I. Shklovskii, Phys. Rev. B **76**, 233402 (2007).
[6] V. M. Pereira, V. N. Kotov, and A. H. Castro Neto, Phys. Rev. B **78**, 085101 (2008).
[7] For a review on graphene, see A. H. Castro Neto, F. Guinea, N. M. R. Peres, K. S. Novoselov, and A. K. Geim, arXiv:0709.1163, Rev. Mod. Phys. (to be published).
[8] W. Greiner, B. Muller, and J. Rafelski, *Quantum Electrodynamics of Strong Fields* (Springer, New York, 1985).
[9] J. H. Chen, C. Jang, M. S. Fuhrer, E. D. Williams, and M. Ishigami, Nat. Phys. **4**, 377 (2008).
[10] D. S. Novikov, Appl. Phys. Lett. **91**, 102102 (2007).
[11] F. Schedin, A. K. Geim, S. V. Morozov, E. W. Hill, P. Blake, M. I. Katsnelson, and K. S. Novoselov, Nat. Mater. **6**, 652 (2007).
[12] S. Y. Zhou, G.-H. Gweon, A. V. Fedorov, P. N. First, W. A. de Heer, D.-H. Lee, F. Guinea, A. H. Castro Neto, and A. Lanzara, Nat. Mater. **6**, 770 (2007).
[13] G. Li, A. Luican, and E. Y. Andrei, arXiv:0803.4016 (unpublished).
[14] C. L. Kane and E. J. Mele, Phys. Rev. Lett. **95**, 226801 (2005); for the latest *ab initio* results, see Y. Yao, F. Ye, X. L. Qi, S. C. Zhang, and Z. Fang, Phys. Rev. B **75**, 041401(R) (2007).
[15] J. Martin, N. Akerman, G. Ulbricht, T. Lohmann, J. H. Smet, K. von Klitzing, and A. Yacoby, Nat. Phys. **4**, 144 (2008).
[16] E. Stolyarova, K. T. Rim, S. Ryu, J. Maultzsch, P. Kim, L. E. Brus, T. F. Heinz, M. S. Hybertsen, and G. W. Flynn, Proc. Natl. Acad. Sci. U.S.A. **104**, 9209 (2007).
[17] D. T. Son, Phys. Rev. B **75**, 235423 (2007).
[18] E. G. Mishchenko, Europhys. Lett. **83**, 17005 (2008).
[19] Z. Q. Li, E. A. Henriksen, Z. Jiang, Z. Hao, M. C. Martin, P. Kim, H. L. Stormer, and D. N. Basov, Nat. Phys. **4**, 532 (2008).
[20] V. P. Gusynin, S. G. Sharapov, and J. P. Carbotte, Phys. Rev. Lett. **96**, 256802 (2006).
[21] The behavior of Friedel oscillations in the massless case is also $\propto r^{-3}$ (at finite chemical potential), V. V. Cheianov and V. I. Falko, Phys. Rev. Lett. **97**, 226801 (2006).
[22] V. N. Kotov, B. Uchoa, and A. H. Castro Neto, Phys. Rev. B **78**, 035119 (2008).
[23] J. González, F. Guinea, and M. A. H. Vozmediano, Nucl. Phys. B **424**, 595 (1994).
[24] V. F. Weisskopf, Phys. Rev. **56**, 72 (1939).
[25] C. Itzykson and J.-B. Zuber, *Quantum Field Theory* (Dover, Mineola, NY, 2005).
[26] T. Ando, A. B. Fowler, and F. Stern, Rev. Mod. Phys. **54**, 437 (1982).